Long-Range $\sigma-\pi$ Interactions in Tetrahydro-*4H*-thiopyran End-Capped Oligo(cyclohexylidenes). Photo-Electron Spectroscopy, ab Initio SCF MO Calculations, and Natural Bond Orbital Analyses

Albert W. Marsman,[†] Remco W. A. Havenith,[†,‡] Sabine Bethke,[§] Leonardus W. Jenneskens,*[,†] Rolf Gleiter,[§] Joop H. van Lenthe,[‡] Martin Lutz,[∥] and Anthony L. Spek[∥]

Debye Institute, Department of Physical Organic Chemistry, Utrecht University, Padualaan 8, 3584 CH Utrecht, The Netherlands, Debye Institute, Theoretical Chemistry Group, Utrecht University, Padualaan 8, 3584 CH Utrecht, The Netherlands, Organisch-Chemisches Institut der Universität Heidelberg, Im Neuenheimer Feld 270, 69120 Heidelberg, Germany, and Bijvoet Center for Biomolecular Research, Crystal and Structural Chemistry, Utrecht University, Padualaan 8, 3584 CH Utrecht, The Netherlands

jennesk@chem.uu.nl.

Received February 12, 2000

Long-range $\sigma-\pi$ interactions in tetrahydro-*4H*-thiopyran end-capped oligo(cyclohexylidenes) were identified by He(I) photoelectron spectroscopy (PES) and ab initio RHF/6-31G* calculations. The vertical ionization energies $I_{v,j}$ of the highest occupied molecular orbitals (MO's) were assigned using Koopmans' theorem ($I_{v,j} = -\epsilon_j$) and by correlation with the ionizations of related reference compounds. The experimental (PES) and theoretical (RHF/6-31G*) results are in good agreement. For tercyclohexylidene derivatives which contain two nonconjugated π-bonds splittings $\Delta I_{v,j}$ of the π-bands in the range from ~0.5 to 0.7 eV ($\Delta-\epsilon_j$ ~0.6 to 0.9 eV). For the bi- and tercyclohexylidene compounds containing two sulfur atoms at their α- and ω-end positions the π-type sulfur lone pair bands [Lp_π(S)] split significantly by $\Delta I_{v,j}$ ~0.3 to 0.4 eV ($\Delta-\epsilon_j$ ~0.3 to 0.4 eV), i.e. $\sigma-\pi$ interactions over distances of ca. 8 and 12 Å, respectively, occur. The magnitude of the interactions and the observed splittings are independent of the anti and syn conformations of the oligo(cyclohexylidene) hydrocarbon skeletons. RHF/6-31G* Natural Bond Orbital analyses reveal that the $H_{ax}-C-C-H_{ax}$ precanonical MO's (PCMO's) centered on the cyclohexyl-type rings are paramount for the relay of the through-bond $\sigma-\pi$ interactions; no through-space $\sigma-\pi$ interactions were identified.

Introduction

It is well established that ground-state electronic interactions in nonconjugated π-systems can occur either through-space (TS) or through-bond (TB).[1] Whereas TS interactions are predominantly governed by the orientation and spatial separation of the interacting functionalities, in the case of TB interactions the number as well as the conformation of intervening sp^3 hybridized carbon−carbon bonds play an important role. TB interactions have been identified in compounds in which π-systems are separated by, for example, either a single sp^3 hybridized carbon atom (homoconjugation)[2] or an odd number of sp^3 hybridized carbon−carbon bonds, viz. aliphatic chains or bonds incorporated in ring and cage systems.[3]

Oligo(cyclohexylidenes) containing a functionality at their α- and/or ω-termini were recently proposed as novel molecular building blocks for supramolecular and functional materials.[4] Since their hydrocarbon skeleton consists of cyclohexyl-type rings interconnected via a sp^2 hybridized olefinic bond, an issue that remains to be addressed is to what extent these frameworks can mediate electronic interactions between functionalities incorporated at their α- and ω-positions. It is noteworthy that the He(I) photoelectron (PE) spectrum of the parent compound 1,1′-bicyclohexylidene (**5**, Chart 1) indicated that its olefinic unit interacts with σ-orbitals that are centered on the cyclohexyl-type rings.[5,6] Recently, ab initio (RHF/6-31G) calculations confirmed this interpretation and enabled the assignment of the orbitals

* To whom correspondence should be addressed. Tel.: +31 302533128. Fax.: +31 302534533.
[†] Department of Physical Organic Chemistry, Utrecht University.
[‡] Theoretical Chemistry Group, Utrecht University.
[§] Organisch-Chemisches Institut der Universität Heidelberg.
[∥] Bijvoet Center for Biomolecular Research, Crystal and Structural Chemistry, Utrecht University.

(1) Hoffmann, R. *Acc. Chem. Res.* **1971**, *4*, 1. Hoffmann, R.; Imamura, A.; Hehre, W. J. *J. Am. Chem. Soc.* **1968**, *90*, 1499.
(2) Winstein, S. *Spec. Publ. Chem. Soc.* **1967**, *21*, 5. Warner, P. M. In *Topics in Nonbenzenoid Aromatic Chemistry*; Hirokawa Publishing Co.: Tokyo, 1977; Vol. 283. Paquette, L. A. *Angew. Chem., Int. Ed. Engl.* **1978**, *17*, 100.
(3) Gleiter, R.; Schäfer, W. *Acc. Chem. Res.* **1990**, *23*, 369. Gleiter, R.; Kissleer, B.; Ganter, C. *Angew. Chem., Int. Ed. Engl.* **1987**, *26*, 1252.
(4) (a) Hoogesteger, F. J.; Havenith, R. W. A.; Zwikker, J. W.; Jenneskens, L. W.; Kooijman, H.; Veldman, N.; Spek, A. L. *J. Org. Chem.* **1995**, *60*, 4375. (b) Hoogesteger, F. J.; Kroon, J. M.; Jenneskens, L. W.; Sudhölter, E. J. R.; de Bruin, T. J. M.; Zwikker, J. W.; ten Grotenhuis, E.; Mareé, C. H. M.; Veldman, N.; Spek, A. L. *Langmuir* **1996**, *12*, 4760. (c) ten Grotenhuis, E.; Marsman, A. W.; Hoogesteger, F. J.; van Miltenburg, J. C.; van der Eerden, J. P.; Jenneskens, L. W.; Smeets, W. J. J.; Spek, A. L. *J. Cryst. Growth* **1998**, *191*, 834 and references cited. (d) Marsman, A. W.; Leusink, E. D.; Zwikker, J. W.; Jenneskens, L. W.; Smeets, W. J. J.; Spek, A. L. *Chem. Mater.* **1999**, *11*, 1484.
(5) Allan, M.; Snyder, P. A.; Robin, M. B. *J. Phys. Chem.* **1985**, *89*, 4900.
(6) Heilbronner, E.; Honegger, E.; Zambach, W.; Schmitt, P.; Günther, H. *Helv. Chim. Acta* **1984**, *67*, 1681.

10.1021/jo000199y CCC: $19.00
Published on Web 06/24/2000

Chart 1. Investigated Oligo(cyclohexylidenes)

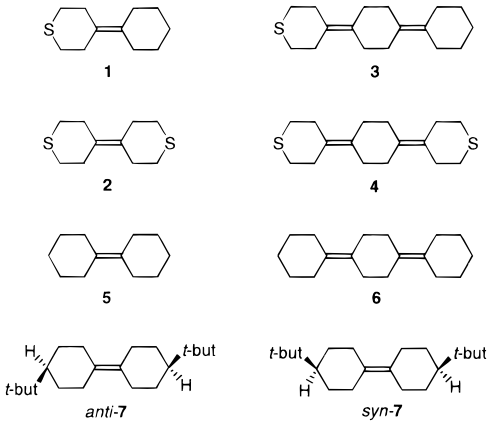

Chart 2. Reference Compounds

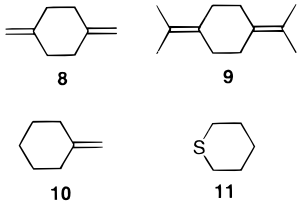

involved.[7] Furthermore, it was shown for 1,1′;4′,1″-tercyclohexylidene (**6**, Chart 1), viz. the next higher homologue, and the reference compounds 1,4-dimethylidenecyclohexane (**8**, Chart 2), for which He(I) photoelectron spectroscopy (PES) results are available,[8] as well as 1,4-diisopropylidenecyclohexane (**9,** Chart 2) that the two π(C═C) units are nondegenerate. Due to TB interactions the π-type HOMO and HOMO-1 are split by ca.0.6 eV. A similar splitting between remote olefinic substituents was identified in the PE spectrum of stella-2,6-diene.[9]

Here we report that in tetrahydro-*4H*-thiopyran end-capped oligo(cyclohexylidenes) (**1**−**4**, Chart 1) $\sigma-\pi$ interactions occur between the 3p-sulfur lone pairs [Lp$_\pi$(S)] positioned at the α and/or ω termini and both σ/π-orbitals located on the oligo(cyclohexylidene) hydrocarbon skeleton; i.e., those involving the olefinic bonds and σ-MO's of appropriate symmetry centered on the cyclohexyl-type rings. In the case of **2** and **4** these $\sigma-\pi$ interactions are mediated over distances of ca. 8 and 12 Å! The occurrence of TB interactions was unequivocally established by measurement of the He(I) PE spectra of oligo(cyclohexylidenes) **1**−**7**. Vertical ionization energies ($I_{v,j}$) of **1**−**7** were assigned by band correlation with He(I) PES data of the reference compounds **8**, **10**, and **11** (Chart 2). The empirical assignments for **1**−**7** were substantiated by comparison of the $I_{v,j}$ values with RHF/6-31G* MO energies (ϵ_j) of the canonical molecular orbitals (CMO's) of each compound applying Koopmans' theorem ($I_{v,j} = -\epsilon_j$).[10] Finally, RHF/6-31G* natural bond orbital (NBO) analyses were executed to identify TS and TB contributions.

Scheme 1. Synthesis of 2 via the Modified Barton−Kellogg Procedure[11]

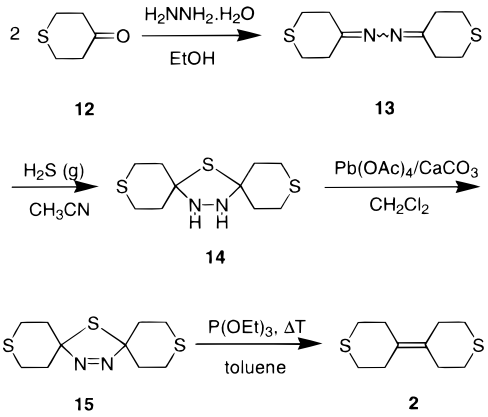

Scheme 2. Synthesis of 4 via a Decarboxylative−Dehydration Route

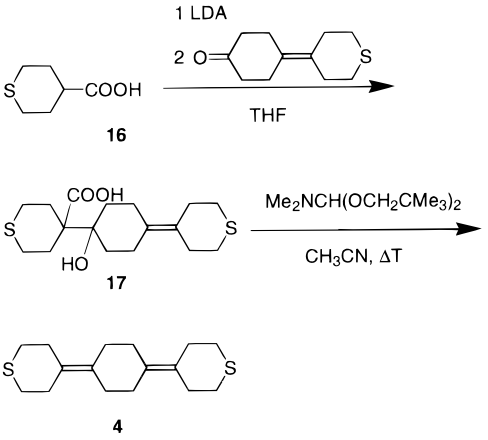

Results and Discussion

Syntheses. 4-(Cyclohexylidene)tetrahydro-*4H*-thiopyran (**1**) and 4-(4-(cyclohexylidene-cyclohexylidene))tetrahydro-*4H*-thiopyran (**3**, Chart 1) were prepared using previously reported procedures.[4a] 4,4′-(Tetrahydro-*4H*-thiopyran-ylidene) (**2**) was obtained in four steps using a 2-fold extrusion methodology.[4a,11] Reaction of 2 equiv *of* tetrahydro-*4H*-thiopyran-4-one (**12**) with $H_2NNH_2 \cdot H_2O$ gave azine **13**, which was treated with H_2S(g) to give thiadiazolidine **14**. The latter was converted into thiadiazoline **15** by oxidation. Subsequently, extrusion of N_2 by heat treatment and with the aid of triethyl phosphite from **15** gave **2** (Scheme 1 and Experimental Section). 4-(Tetrahydro-*4H*-thiopyran-4-cyclohexylidene-4′-ylidene-)tetrahydro-*4H*-thiopyran (**4**) was prepared using similar procedures as for the syntheses of **1** and **3**. Tetrahydro-*4H*-thiopyran-4-carboxylic acid (**16**)[12] was coupled with 4-(tetrahydro-*4H*-thiopyran-4-ylidene)cyclohexanone, viz. an intermediate product in the synthesis of **3**,[4] furnishing β-hydroxy acid **17**. The latter was converted into **4** by treatment with *N*,*N*-dimethylformamide dineopentyl acetal (Scheme 2 and Experimental Section).

Ground-State Conformational Properties of 1−6. In line with the behavior of the reference compounds **8**

(7) Havenith, R. W. A.; van Lenthe, J. H.; Jenneskens, L. W.; Hoogesteger, F. J. *Chem. Phys.* **1997**, *225*, 139.
(8) Heilbronner, E.; Schmelzer, A. *Helv. Chim. Acta* **1975**, *58*, 936.
(9) (a) Gleiter, R.; Lange, H.; Borzyk, O. *J. Am. Chem. Soc.* **1996**, *118*, 4889. (b) Lange, H.; Gleiter, R.; Fritzsche, G. *J. Am. Chem. Soc.* **1998**, *120*, 6563.
(10) Koopmans, T. *Physica* **1934**, *1*, 104.
(11) (a) Barton, D. H. R.; Willis, B. J. *J. Chem. Soc, Perkin Trans. 1* **1972**, 305. (b) Buter, J.; Wassenaar, S.; Kellogg, R. M. *J. Org. Chem.* **1972**, *3*, 7, 4045.
(12) Strässler, S.; Linden, A.; Heimgartner H. *Helv. Chim. Acta* **1997**, *80*, 1528.

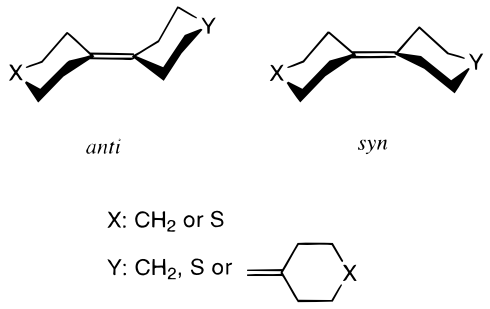

Figure 1. Schematic representation of the different possible conformers of **1**−**6**.

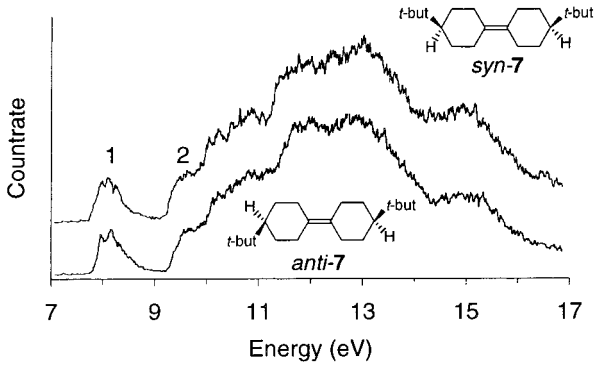

Figure 2. He(I) photoelectron spectra of *anti*-**7** and *syn*-**7**.

and **9** (Chart 2),[13] temperature-dependent ^{1}H NMR ($CDCl_3$) spectroscopy showed that the cyclohexyl-type rings of **1**−**6** are conformationally mobile in solution (see Experimental Section).[4] The interconnected chairlike, cyclohexyl-type rings can adopt either an anti or syn conformation with respect to each other (Figure 1). Ab initio calculations revealed that *anti*-**5** and *syn*-**5** are both genuine minima and possess a nearly identical total energy [RHF/6-31G*; $\Delta E_{tot} = E_{tot}$(syn) − E_{tot}(anti) −0.007 kcal/mol]; both in the gas phase and in solution an equilibrium mixture of the conformers (ratio ca. 1:1) is expected.[14] It is noteworthy that the ϵ_j values as well as the character of the highest occupied MO's of *anti*-**5** and *syn*-**5** are virtually identical. This was verified by a comparison of the He(I) PE spectra of *anti*- (*anti*-**7**) and *syn*-4,4′-*tert*-butyl-1,1′-bicyclohexylidene (*syn*-**7**), viz. conformationally stable derivatives of **5** [**7**; $\Delta E_{tot} = E_{tot}$(syn) − E_{tot}(anti) −0.088 kcal/mol, Chart 1 and Figure 2].[15] Their PE spectra are similar and closely resemble that of **5** (Figures 2 and 4 and Table 2).[5] These results suggest that also in the case of **1**−**4** and **6** the He(I) PE spectra will originate from mixtures of conformers (**1** and **2**; *anti*- and *syn*-**3**;[16] anti/anti, syn/anti, anti/syn and syn/syn, and, **4** and **6**; anti/anti, anti/syn and syn/syn, Figure 1). To establish if a similar conformational independence holds for the ϵ_j values and the character of the highest occupied MO's of the different conformers of **1**−**4** and **6**, their conformers were studied using ab initio methods (see Experimental Section). Since **1**−**4** contain sulfur, the use of polarization functions is required. Consequently, all conformers were optimized with a RHF/6-31G* basis set. The results obtained for the distinct conformers of each compound, which were all shown to be genuine minima, revealed that the ϵ_j values and the character of the highest occupied MO's were virtually identical. This is exemplified for **1** and **2** in Table 3 and **6** in Table 2 (for **3** and **4** see Table 1 of the Supporting Information). For each compound, the ΔE_{tot} values of each conformers with respect to that with the lowest E_{tot} are less than 0.15 kcal/mol. Hence, in the gas phase, mixtures of conformers are expected. Since the anti and anti/anti conformer of **5** and **6**, respectively, were previously studied at the RHF/6-31G level of theory,[7] they were also re-optimized with a 6-31G* basis set; similar results were obtained. In addition, for **6** its anti/syn and syn/syn conformers were also calculated at the 6-31G* level of theory. For all conformers again nearly identical results were obtained (Table 2).

The effect of basis set size was assessed for *anti*-**1**, *anti*-**2**, and *syn*-**2**, i.e. the calculations were repeated with a 6-311G** basis set. Although the RHF/6-311G** ϵ_j values are ca. 0.06 eV larger than the corresponding

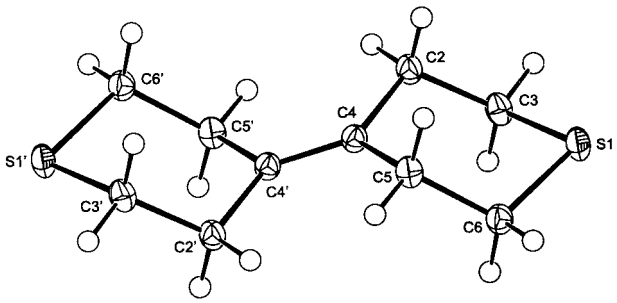

Figure 3. Displacement ellipsoid plot of **2** (50% probability level; symmetry operation′: $1 - x$, $1 - y$, $1 - z$).

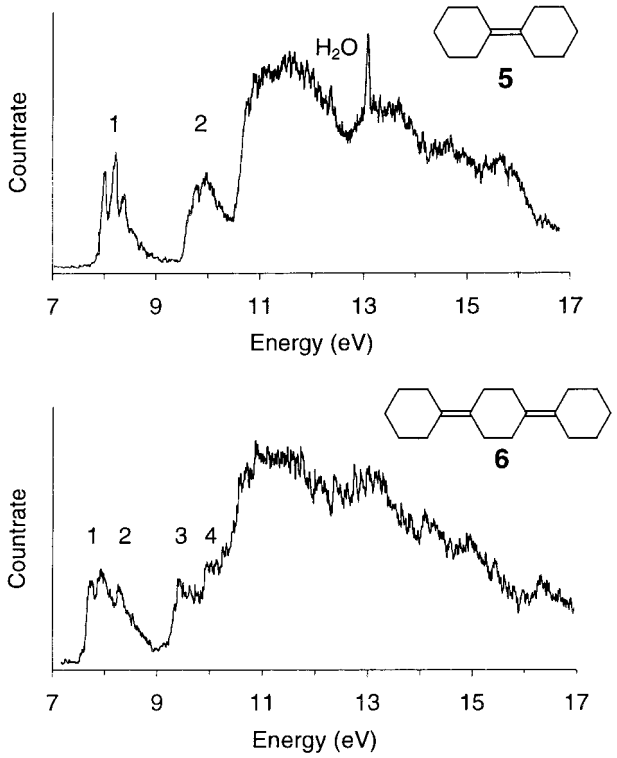

Figure 4. He(I) photoelectron spectra of **5** and **6**.

(13) Lautenschläger F.; Wright; G. F. *Can. J. Chem.* **1963**, *41*, 1972. Lambert, J. B. *J. Am. Chem. Soc.* **1967**, *89*, 67.

(14) Havenith, R. W. A.; Jenneskens, L. W.; van Lenthe, J. H., *Chem. Phys. Lett.* **1998**, *282*, 39.

(15) Due to the preference of the *tert*-butyl substituents to occupy an equatorial position both *anti*-**7** and *syn*-**7** are conformationally stable.[11b]

(16) The first designated bicyclohexylidene unit contains the sulfur atom.

Table 1. Salient Features of the Single-Crystal X-ray and RHF/6-31G* (6-311G) Structure of *anti*-2**

structural parameter	single-crystal X-ray structure	RHF/6-31G* (6-311G**) structure
bond lengths (Å)		
C4−C4′	1.343(3)	1.334 (1.333)
C2−C4/C5−C4	1.5167(19)/1.5123(18)	1.520 (1.520)
C2−C3/C5−C6	1.528(2)/1.526(2)	1.534 (1.533)
C3−S1/C6−S1	1.8067(15)/1.8071(15)	1.815 (1.820)
valence angles (deg)		
C3−S1−C6	97.16(7)	98.5 (98.6)
C2−C4−C5	111.48(11)	110.9 (111.0)
C3−C2−C4/C4−C5−C6	112.57(12)/113.28(12)	112.1 (112.3)
C2−C4−C4′/C5−C4−C4′	123.95(15)/124.57(15)	124.6 (124.5)
C2−C3−S1/C5−C6−S1	112.33(10)/112.40(10)	113.0 (112.9)
dihedrals angles (deg)		
C2−C4−C4′−C5′	−0.4(3)	−0.34 (−1.20)
C2−C4−C4′−C2′	180.0(7)	−180 (−180)
C3−C2−C4−C5/C6−C5−C4−C2	60.79(16)/−60.45(15)	64.1 (64.0)
C3−C2−C4−C4′/C6−C5−C4−C4′	−118.91(19)/119.2(2)	−114.5 (−114.9)
C4−C2−C3−S1/C4−C5−C6−S1	−62.76(14)/61.74(14)	61.4 (61.3)
C6−S1−C3−C2/C5−C6−S1−C3	55.11(11)/−54.42(11)	51.1 (51.0)

[a] For atom numbering see figure 3.

Table 2. PES Vertical Ionization Energies $I_{v,j}$ (eV), RHF/6-31G* Orbital Energies $-\epsilon_j$ (eV), and Their Assignments of *anti*-5 (C_{2h}), *anti/anti*-6 (C_{2h}), *anti*-7 (C_{2h}), and *syn*-7 (C_{2v})[a-c]

compd	band j	$I_{v,j}$	$-\epsilon_j$	assignment
anti-**5**[14]	1	8.16	8.58	$14b_u\,\pi$
	2	9.80	11.00	$9b_g\,\sigma$
syn-**5**[14]	1		8.58	$15a_1\,\pi$
	2		11.00	$9a_2\,\sigma$
anti/anti-**6**	1	7.88[d]	8.35	$21a_g\,\pi^+$
	2	8.34	8.91	$20b_u\,\pi^-$
	3	9.60	10.86	$13b_g\,\sigma$
	4	10.2	11.42	$14a_u\,\sigma$
anti/syn-**6**	1		8.36	$41a'\,\pi^+$
	2		8.91	$40a'\,\pi^-$
	3		10.86	$27a''\,\sigma$
	4		11.42	$26a''\,\sigma$
syn/syn-**6**	1		8.37	$21a_g\,\pi^+$
	2		8.91	$20b_u\,\pi^-$
	3		10.87	$13b_g\,\sigma$
	4		11.42	$14a_u\,\sigma$
anti-**7**	1	8.04	8.56	$24b_u\,\pi$
	2	9.50	10.81	$15b_g\,\sigma$
syn-**7**	1	8.07	8.56	$25a_1\,\pi$
	2	9.50	10.82	$15a_2\,\sigma$

[a] In addition, RHF/6-31G* $-\epsilon_j$ (eV) values and their assignments of *syn*-**5** (C_{2v}), *anti/syn*-**6** (C_s), and *syn/syn*-**6** (C_{2h}) are presented. [b] E_{tot}: *anti*-**5** −466.064786 au, *syn*-**5** −466.064797 au, *anti/anti*-**6** −697.921586 au, *anti/syn*-**6** −697.921597 au, *syn/syn*-**6** −697.921608 au, *anti*-**7** −778.304855 au, and *syn*-**7** −778.304869 au (1 au = 627.52 kcal/mol). [c] $\Delta E_{tot} = E_{tot}(\text{syn}) - E_{tot}(\text{anti})$: **5** −0.007 kcal/mol and **7** −0.088 kcal/mol. For **6** $\Delta E_{tot} = E_{tot}(syn/syn) - E_{tot}(x)$: *anti/anti*-**6** −0.014 kcal/mol and *anti/syn*-**6** −0.007 kcal/mol. [d] Average value of the discernible peaks at 7.82 and 7.94 eV.

RHF/6-31G* values, the relative energies and the character of the highest occupied MO's do not change (Table 3).

Single-Crystal X-ray Structure of 2. The RHF/6-31G* geometries[7] of *anti*-**5** and *anti*-**6** are in satisfactory agreement with the single-crystal X-ray structural data of **5** and *trans*-4,4″-diheptyl-1,1′:4′,1″-tercyclohexylidene,[17] respectively. To verify that the structural features of **1**−**4** are adequately reproduced with both the 6-31G* and the 6-311G** basis set, the optimized geometries of *anti*-**2** were compared with its single-crystal X-ray structure (C_i; approximate C_{2h}). As shown by the salient bond lengths, valence angles and dihedral angles, the RHF/6-31G* and RHF/6-311G** calculations satisfactorily reproduce the single-crystal X-ray structural data (Table 1 and Figure 3).[18,19]

Photoelectron Spectroscopy of 1−6. To establish if in the case of **1**−**6** ground-state interactions are relayed via the oligo(cyclohexylidene) $\sigma-\pi$ hydrocarbon skeleton, their He(I) PE spectra were measured (Figures 4−7). The recorded vertical ionization energies ($I_{v,j}$) are collected in Tables 2 and 3. Empirical assignment of the $I_{v,j}$ values below ca. 10 eV, which are separated from the high energy σ-MO manifold, was achieved by band-shape analysis as well as band correlation between structurally related derivatives.

To discuss the PE spectra of **1**−**6** we first focus on those of **8**, **10**, and **11** to estimate the ionization energies of the unperturbed 3p-sulfur lone pair [Lp_π(S)] (**11**) and the exo-cyclic olefinic bond (**10**) as well as the interaction of two double bonds in 1,4-dimethylidenecyclohexane (**8**). The PE spectrum of **10** shows one band at 9.13 eV with vibrational fine structure ($\nu \approx 1330$ cm^{-1}).[20] It is assigned to ionization from the π-orbital. This band is shifted approximately 1 eV toward lower energy in the PE spectrum of **5** (8.16 eV, Figure 4).[5] The vibrational fine structure ($\nu \approx 1450$ cm^{-1}) is similar to that found for **10**. In the PE spectrum of **7** a further shift of the first band toward lower energy was observed (Table 2). In the PE spectrum of **8** two clearly separated bands at 9.0 and 9.4 eV have been reported.[20] A similar gap (0.4−0.8 eV) was also found for several bridged derivatives.[21]This splitting between the two bands has been interpreted as being due to a considerable TB interaction with the ribbon-type orbitals of the six-membered ring.[22]

(17) Suitable single crystals for X-ray analysis could hitherto not be obtained for **6**.

(18) In the solid-state **2**, like **5**, possesses an *anti*-type structure with crystallographic C_i and noncrystallographic, approximate C_{2h} symmetry. Crystallographic details for **2** are presented in the Supporting Information. Cf. also Veldman, N.; Spek, A. L.; Hoogesteger, F. J.; Zwikker, J. W.; Jenneskens, L. W. *Acta Crystallogr.* **1994**, *C50*, 742.

(19) No bond length alternations are found in the sp^3-sp^3 carbon−carbon bonds of the cyclohexyl-type rings of **2**; cf. Baldridge, K. K.; Battersby, T. R.; Vernonclark, R.; Siegel, J. S. *J. Am. Chem. Soc.* **1997**, *119*, 7048.

(20) Bieri, G.; Binger, F.; Heilbronner, E.; Maier, J. P. *Helv. Chim. Acta* **1977**, *60*, 2213.

(21) Chou, T.-C.; Lange, H.; Gleiter, R.; Gögh, T.; Kriz, M.; Pfenninger, R. H.; Valentiuy, M.; Ganter, C. *Helv. Chim. Acta* **1995**, *28*, 2011.

(22) Hoffman, R.; Mollère, P. D.; Heilbronner, E. *J. Am. Chem. Soc.* **1973**, *95*, 4860.

Table 3. Vertical Ionization Energies $I_{v,j}$ (eV), RHF/6-31G* Orbital Energies $-\epsilon_j$ (eV) and Assignments of *anti*-1 (C_s), *syn*-1 (C_s), *anti*-2 (C_{2h}), *syn*-2 (C_{2v}), *anti/anti*-3 (C_s), and *anti/anti*-4 (C_{2h})[a-c]

Compound	Band	$I_{v,j}$	$-\epsilon_j$		Assignment	
	j		*anti*	*syn*	*anti*	*syn*
1	1	8.16	8.66 (8.73)	8.67	31a' $\pi/Lp_\pi(S)$	31a' $\pi/Lp_\pi(S)$
	2	8.63	9.19 (9.25)	9.19	30a' $Lp_\pi(S)/\pi$	30a' $Lp_\pi(S)/\pi$
	3	9.95	11.29 (11.33)	11.29	19a'' $Lp_\sigma(S)$	19a'' $Lp_\sigma(S)$
			11.33 (11.37)	11.32	29a' σ	29a' σ
2	1	8.27	8.76 (8.84)	8.82 (8.91)	$17b_u$ $\pi/Lp_\pi(S)$	$18a_1$ $\pi/Lp_\pi(S)$
	2	8.49	9.12 (9.18)	9.07 (9.12)	$17a_g$ $Lp_\pi(S)$	$16b_2$ $Lp_\pi(S)$
	3	8.89	9.53 (9.59)	9.55 (9.60)	$16b_u$ $Lp_\pi(S)/\pi$	$17a_1$ $Lp_\pi(S)/\pi$
	4	10.4	11.49 (11.54)	11.37 (11.41)	$16a_g$ $Lp_\sigma(S)$	$15b_2$ $Lp_\sigma(S)$
		10.9	11.51 (11.56)	11.59 (11.63)	$15b_u$ $Lp_\sigma(S)$	$10a_2$ $Lp_\sigma(S)$
			11.59 (11.63)	11.65 (11.70)	$10b_g$ σ	$16a_1$ σ
			anti/anti		*anti/anti*	
3	1	~8.3	8.48		44a' π	
	2		8.88		43a' $Lp_\pi(S)/\pi$	
	3	8.65	9.29		42a' $\pi/Lp_\pi(S)$	
	4		11.05		28a'' σ	
			11.33		41a' $Lp_\sigma(S)$	
			11.66		27a'' σ	
4	1		8.60		$24a_g$ $\pi/Lp_\pi(S)$	
	2	8.0-8.5	8.89		$23b_u$ $Lp_\pi(S)/\pi$	
	3		9.21		$23a_g$ $Lp_\pi(S)/\pi$	
	4	~8.6	9.49		$22b_u$ $\pi/Lp_\pi(S)$	
	5	10.2	11.28		$14b_g$ $Lp_\sigma(S)$	
	6	10.9	11.40		$21b_u$ $Lp_\sigma(S)$	
			11.42		$22a_g$ σ	
			11.88		$15a_u$ σ	

[a] RHF/6-311G** values in parentheses. [b] E_{tot}: *anti*-**1** −824.537362 au (RHF/6-311G** −824.658005 au), *syn*-**1** −824.537353 au, *anti*-**2** −1183.009415 au (RHF/6-311G** −1183.144416 au), *syn*-**2** −1183.009285 au (RHF/6-311G** −1183.144179 au), *anti/anti*-**3** −1056.394149 au and *anti/anti*-**4**-1414.866488 au (1 au = 627.52 kcal/mol). [c] $\Delta E_{tot} = E_{tot}$(anti) − E_{tot}(syn): **1** −0.006 kcal/mol and **2** −0.082 (−0.149) kcal/mol.

In the PE spectrum of **6** we observe one broad feature centered around 8 eV to which we assign ionizations out of the two π-orbitals of **6** (Figure 4). Assuming a similar vibrational fine structure as for **5** we ascribe the first two peaks at 7.82 and 7.94 eV to the vibrational progression of the first band, while the peak at 8.34 eV must consequently be assigned to a second band. The splitting of the two bands (0.46 eV) is in the same order of magnitude as observed for **8** and its bridged congeners.[21]

In the PE spectrum of **1** two bands below 9 eV are found at 8.16 and 8.63 eV (Figure 5). The second band is sharper than the first one. We assign the first one to the ionization from the π-orbital, the second one to the ionization from the $Lp_\pi(S)$ orbital. This assignment is corroborated by comparing the PE spectrum of **1** with that of **5** and of tetrahydro-*4H*-thiapyrane (**11**).[23,24] In the latter molecule the first ionization energy of the 3p-sulfur lone pair was found at 8.45 eV. The three bands in the PE spectrum of **2** at 8.27, 8.49, and 8.89 eV are assigned to ionizations from the π-orbital and the two symmetry adapted $Lp_\pi(S)$ combinations b_u and a_g. This conclusion is confirmed by comparing the PE data of **1**, **2**, and **5** as shown in Figure 6.

The qualitative interpretation of the PE spectra of **3** and **4** (Figure 7) is less straightforward. The PE spectrum of **3** shows two broad features centered around 8.3 and 8.65 eV. A comparison with the first ionization energies of **6** and **11**[23,24] indicates that these two broad features consists of three transitions (bands 1−3). In the PE

(23) Gleiter, R.; Spanget-Larsen, J. In *Topics in Current Chemistry*; Springer-Verlag: Berlin Heidelberg, New York, 1979; *86*, 139 and references cited.

(24) Sweigart, D. A.; Turner, D. W. *J. Am. Chem. Soc.* **1972**, *94*, 5599.

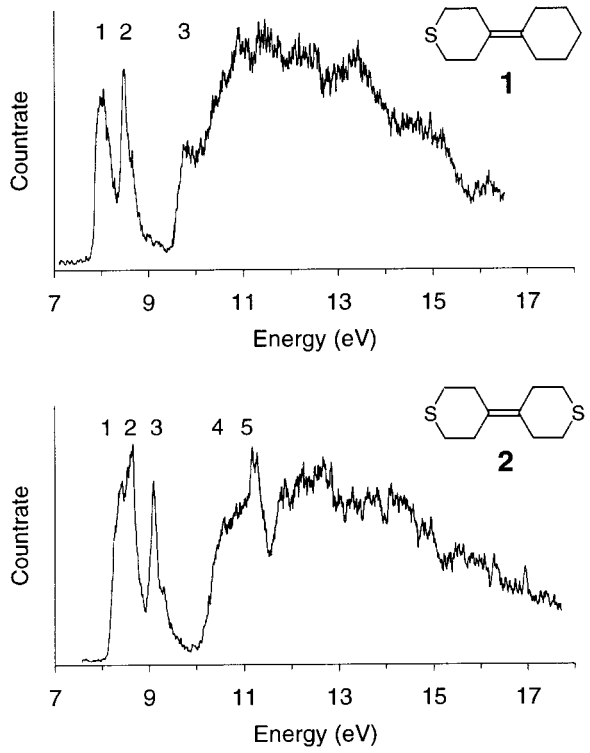

Figure 5. He(I) photoelectron spectra of **1** and **2**.

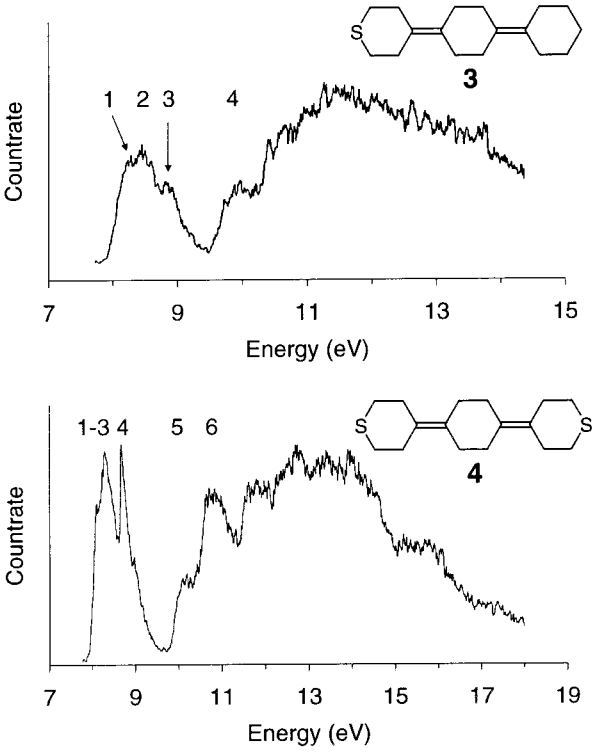

Figure 7. He(I) photoelectron spectra of **3** and **4**.

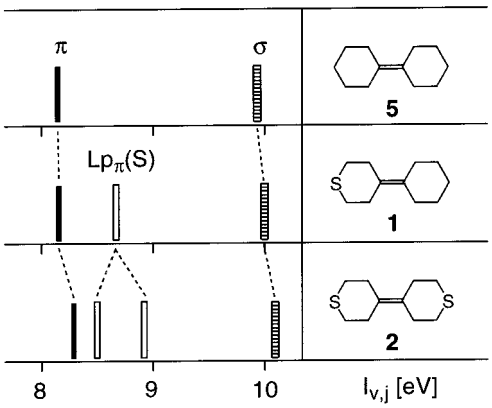

Figure 6. Schematic correlation diagram of the first ionization energies, $I_{v,j}$, of **1**, **2**, and **5**. For detailed band assignments (RHF/6-31G* calculations) see Tables 2 and 3.

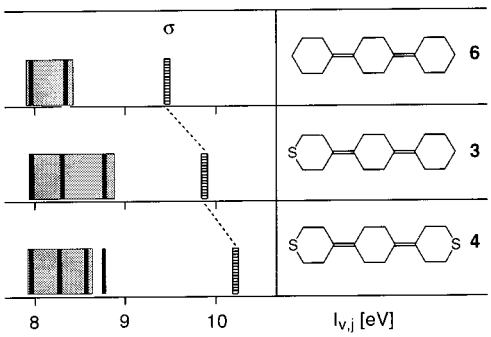

Figure 8. Schematic correlation diagram of the first ionization energies, $I_{v,j}$, of **3**, **4**, and **6**. For detailed band assignments (RHF/6-31G* calculations) see Tables 2 and 3.

spectrum of **4** two peaks are observed below 9 eV; one broad (8.0−8.5 eV) centered around 8.3 eV and a second sharp one at ∼8.6 eV. A comparison with the PE data of **3** and **6** accordingly suggests assigning four transitions to both peaks. The steep onset of the second peak (8.62 eV) suggests that it has to be ascribed to the ionization from a $Lp_{\pi}(S)$ orbital combination. In both the PE spectra of **3** and **4** the bands of the individual transitions show overlap, which is too strong to further discriminate. In Figure 8 the first bands of **3**, **4** and **6** are compared.

The assignment of the PE data of **1**−**6** presented in Tables 2 and 3 was further supported by a comparison of the experimental ionization energies ($I_{v,j}$) with calculated orbital energies by using the HF−SCF procedure with a 6-31G* basis set[25] and applying Koopmans' theorem ($I_{v,j} = -\epsilon_j$).[10]

The energy difference between the first two bands in **6** (0.46 eV) is reproduced quite well by the calculations (0.56 eV). The same holds for the first two bands in the PE spectrum of **1** (PES, 0.47 eV and RHF/6-31G*: *anti*-**1**, 0.53 eV, *syn*-**1**, 0.52 eV). For **2** the measured energy gaps between the first three bands (0.22 and 0.40 eV) are reproduced fairly well by the calculations in both of its conformations [*anti*-**2** (C_{2h}), 0.36 and 0.41 eV or *syn*-**2** (C_{2v}), 0.25 and 0.48 eV].

In the case of *anti*/*anti*-**3** (C_s) the calculation predicts three bands positioned at 8.48, 8.88, and 9.29 eV in the PE spectrum. Unfortunately, only a broad band is observed. The occurrence of band overlap might be rationalized by the presence of a mixture of conformers in the gas phase at the recording temperature (125 °C). For **4** the calculation predicts small energy differences (ca. 0.3 eV) for the four highest occupied orbitals. Only the very sharp peak (band 4; ∼8.6 eV) is clearly separated from the first broad peak (Figure 7, Table 3 and see the Supporting Information).

Analysis of σ−π Interactions in 1−6. The electronic interactions in **1**−**6** were further analyzed on the basis of the concept of through-space (TS) and through-bond (TB) interactions introduced by Hoffmann et al.;[1] a

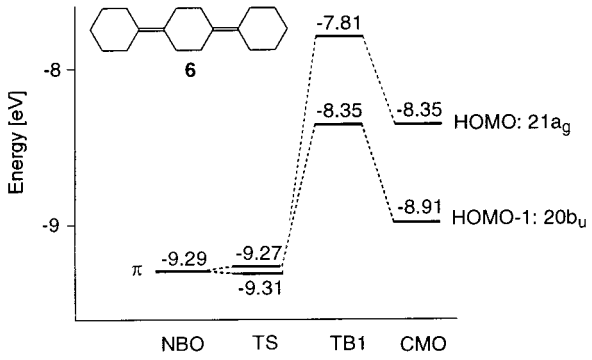

Figure 9. Through-space (TS) and through-bond (TB) interaction diagram of **6**: NBO, self-energy of the π-NBO's; TS, energy after the TS interaction; TB1, energy after the TB interaction with the σ-orbitals shown in Figure 11; CMO, energy of the CMO's.

methodology first suggested by Heilbronner and Schmelzer is used.[8] For a quantitative treatment the procedure of Imamura et al.[26] is applied using Weinhold's natural bond orbitals[27] (NBO's) as a starting point. The analysis is based on the Fock matrix in a localized basis of the one-electron wave functions and comprises a transformation of the Hartree−Fock canonical molecular orbitals (CMO's) into a set of localized MO's called natural bond orbitals (NBO's).[27] Subsequently, diagonalization of a sub-matrix of the nondiagonal NBO Fock matrix results in a set of precanonical MO's (PCMO's), which possess eigenvalues corresponding to the MO energies after interaction of the NBO's within that specific sub-matrix.

In the case of **5** the NBO analysis reveals a self-energy for the π-orbital of −9.28 eV (not shown). This level is significantly destabilized by interaction with a precanonical MO (PCMO) comprising of four $H_{ax}-C-C-H_{ax}$ and the two $C-H_{eq}$ NBO's of the cyclohexyl-type rings (Figure 11). For the interaction of **6** the NBO analysis reveals that TS interaction between both degenerate π-NBO's is minute; the TS splitting between the symmetry-adapted linear combinations of both π-NBO's [π^+ (a_g) and π^- (b_u)][28] is negligible ($\Delta-\epsilon_j$ 0.04 eV, Figure 9). This is expected on the basis of their through-space separation (3 Å)[29] and is confirmed by ghost-atom calculations.[30] Like the π-NBO of **5**, interaction with a PCMO comprising six $H_{ax}-C-C-H_{ax}$ and two $C-H_{eq}$ NBO's destabilizes the π^+- and π^- combinations of **6** (TB1) in such a way that π^+ is placed on top of π^- in accordance with the occurrence of TB interactions over an odd number of intervening sp^3 hybridized carbon−carbon bonds. A splitting of the resulting PCMO's of $\Delta-\epsilon_j$ 0.54 eV is found, which is close to that of the related CMO's ($\Delta I_{v,j}$ 0.46 eV and $\Delta-\epsilon_j$ 0.56 eV). Additional admixture of other σ-NBO's does not significantly affect this splitting.[31] The NBO analyses show that TB $\sigma-\pi$ interactions indeed involve the $H_{ax}-C-C-H_{ax}$ PCMO's (Figure 11). While the $H_{ax}-C-C-H_{ax}$ PCMO responsible for the splitting of the π-NBO's of **6** is that positioned in the middle cyclohexyl-type ring, those located in the outer rings mainly destabilize their neighboring π-NBO. However in going from **5** and **6** to **1**−**4**, the terminal (α and/or ω) methylene units are replaced by sulfur atoms of which the Lp_π(S) NBO's possess a favorable energy and

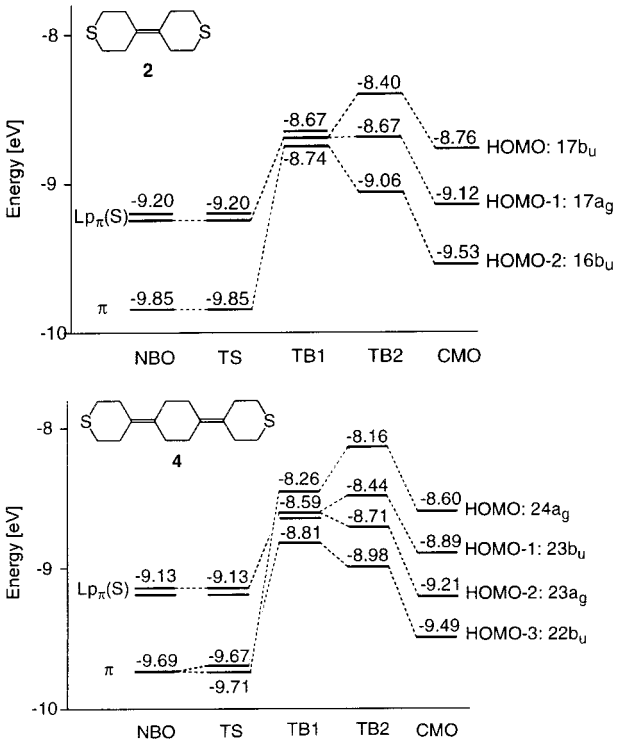

Figure 10. Through-space (TS) and through-bond (TB) interaction diagram of **2** and **4**: NBO, self-energy of the π- and Lp_π(S) NBO's; TS, energy after TS interaction; TB1, energy after the interaction of either the π- or the Lp_π(S) NBO's with the σ-orbitals shown in Figure 11; TB2, energy after simultaneous interaction of the π- and Lp_π(S) NBO's with the σ-orbitals; CMO, energy of the CMO's.

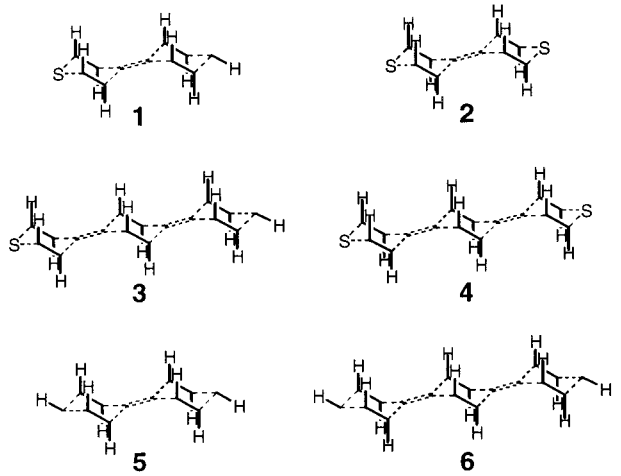

Figure 11. Schematic representation of the σ-orbitals considered in the through-bond interactions (TB1 and TB2).

(25) Hariharan, P. C.; Pople, J. A. *Theor. Chim. Acta* **1973**, *28*, 213.
(26) Imamura, A.; Ohsaku, M. *Tetrahedron* **1981**, *37*, 2191.
(27) Reed, A. E.; Weinhold, F. *J. Chem. Phys.* **1983**, *78*, 4066. Reed, A. E.; Weinstock, R. B.; Weinhold, F. *J. Chem. Phys.* **1985**, *83*, 735.
(28) The π^+ combination is symmetrical with respect to the molecular C_2 axis.[1]
(29) Paddon-Row, M. N.; Wong, S. S.; Jordan, K. D. *J. Chem. Soc., Perkin Trans. 2* **1990**, 425.
(30) RHF/6-31G calculations on a system consisting of two ethene molecules located at the position of the π-bonds in the optimized geometry of *anti*/*anti*-**6** augmented by ghost centers, viz. the proper basis functions without nuclei on all other atomic positions discernible for **6**, show that under these conditions the π-bonds are nearly degenerate.[7]
(31) Admixture of the *anti*-bonding PCMO's of the $H_{ax}-C-C-H_{ax}$ units causes a stabilization of the PCMO's towards the levels of the CMO's.

belong to the appropriate irreducible representation[23] for interaction with the outer ring $H_{ax}-C-C-H_{ax}$ PCMO. Hence, the Lp_π(S) NBO's will perturb the MO topologies of **5** and **6**.

The NBO analyses for **1**−**4** reveal different basis orbitals for the localized π-unit and the Lp_π(S) NBO's, which is shown for **2** and **4** on the left side of Figure 10. TS interactions between the Lp_π(S) and π-NBO's is insignificant in all cases (NBO/TS, Figure 10). In the case of **2** and **4** no sizable splitting between the Lp_π(S) or the π-orbitals in **4** is observed. This is in line with the TS separation of the sulfur- and nearest π-bond carbon atoms [d(S1···C4) = 3.2 Å, **2**].[32] The situation changes if TB interaction occur (TB1 and TB2). In the case of **2** the interaction of a PCMO comprising of four $H_{ax}-C-C-H_{ax}$ NBO's of the σ-skeleton with either the Lp_π(S) NBO's or the π-NBO's causes a considerable destabilization of the 3p-sulfur lone pairs and the π-orbital (TB1 Figure 10). Subsequently, in the TB2 step, simultaneous interaction of the aforementioned units causes the Lp_π(S) NBO's to split. In the case of **4** interaction of either the π- or Lp_π(S) NBO's with a PCMO comprising of six $H_{ax}-C-C-H_{ax}$ NBO's not only results in a destabilization of the π- and 3p-sulfur lone pairs, but also in a splitting of the symmetry adapted π-orbitals [$a_g(\pi^+)$ and $b_u(\pi^-)$] by 0.55 eV (Figure 10). In the next step (TB2) the interaction between the lone pairs at sulfur and the π-orbital(s) occurs. The splittings obtained after the TB2 step in **2** and **4** are about the same as found for the canonical MOs (right side of Figure 10).

The NBO analyses for the less symmetric cases **1** and **3** yield analogous results (not shown). The TB interaction is mainly due to the PCMO's shown in Figure 11. After interaction of the semilocalized π- and Lp_π(S) orbitals the energy differences are close to those calculated for the canonical MO's.

Conclusions

The PES and RHF/6-31G* data show that ground-state electronic interactions between the Lp_π(S)- and/or π-MO's of **1**−**6** occur. For **3**, **4** and **6** this leads to splitting of the π-MO's **3**: $\Delta I_{v,j} \sim 0.7$ (estimated from bandwidth) and $\Delta-\epsilon_j = 0.81$ eV, **4**: $\Delta I_{v,j} \sim 0.6$ (estimated from bandwidth) and $\Delta-\epsilon_j = 0.89$ eV and **6**: $\Delta I_{v,j} = 0.46$ and $\Delta-\epsilon_j = 0.56$ eV). Moreover, in case of **2** and **4**, which both contain sulfur atoms at their termini, the Lp_π(S) MO's are also significantly split [**2**: $\Delta I_{v,j} = 0.40$ eV and $\Delta-\epsilon_j = 0.41$ eV and **4**: $\Delta I_{v,j} \sim 0.3$ eV (estimated using the two band maxima) and $\Delta-\epsilon_j = 0.32$ eV]. Hence, the interactions between Lp_π(S) are efficiently mediated over lengths of 8−12 Å.

RHF/6-31G*/NBO analyses on **1**−**6** show that TB interactions occur and that the $H_{ax}-C-C-H_{ax}$ PCMO's of the cyclohexyl-type rings play a dominant role. The RHF/6-31G* results of the different conformers of **1**-**6** in combination with the He(I) PES results of conformationally locked *anti*- and *syn*-**7** show that the conformation of the hydrocarbon skeleton does not affect the magnitude of the TB coupling, viz. the $H_{ax}-C-C-H_{ax}$ PCMO's can be combined with π-type orbitals within all point groups (C_{2h}, C_s, or C_{2v}) of the studied end-functionalized bi- and tercyclohexylidenes.

(32) The calculated (RHF/6-31G*) Lp_π(S) MO's of a model system consisting of two dimethyl sulfide and one ethene molecule in the geometry of **2** and ghost centers on the missing carbon atoms are nearly degenerate (HOMO, −9.22 eV and HOMO-1, −9.29 eV).[30]

Experimental Section

General Methods. Melting points are uncorrected. NMR spectra (^{1}H 300.133 MHz and ^{13}C 75.47 MHz) are recorded in $CDCl_3$ unless otherwise stated; chemical shifts (ppm) are reported downfield from TMS. Raman spectra were recorded for neat solids. Elemental analyses were performed by Dornis U. Kolbe, Microanalytisches Laboratorium, Mülheim a.d. Ruhr, Germany. Dry THF and CH_2Cl_2 were prepared by distillation from Na and $CaCl_2$, respectively. CH_3CN was dried by storage on 3 Å molecular sieves.

Syntheses. 4-(Cyclohexylidene)tetrahydro-*4H*-thiopyran **(1)** and 4-(4-(cyclohexylidenecyclohexylidene)tetrahydro-*4H*-thiopyran **(3)**[4a] as well as *anti*- (*anti*-**7)** and *syn*-4,4′-*tert*-butyl-1,1′-bicyclohexylidene (*syn*-**7**)[11b] were synthesized according to literature procedures.

4,4′-Bis(tetrahydro-*4H*-thiopyranylidene) (2). A solution of **15** (3.39 g, 13.0 mmol) and triethyl phosphite (12.0 mL, 70 mmol) in toluene (200 mL) was heated at reflux temperature for 24 h. After cooling of the reaction mixture, the solvent was removed in vacuo and the solid residue triturated with CH_3OH (25 mL). The solid was filtered off and, subsequently, sublimed (80 °C, 0.1 Torr) to give pure **2** (1.93 g, 0.63 mmol, 74%): mp 144.1 °C; ^{1}H NMR δ 2.55−2.59 (m, 8H), 2.63−2.67 (m, 8H) ppm; ^{13}C NMR δ 30.6, 31.9, 129.6 ppm; Raman ν 2958, 2945, 2891, 2838, 1661, 1652, 1643, 1453, 1424, 1420 cm^{-1}. Anal. Calcd for $C_{10}H_{16}S_2$: C, 59.98; H, 8.06; S, 31.96. Found: C, 60.11; H, 8.01.

4-(Tetrahydro-*4H*-thiopyran-4-cyclohexylidene-4′-ylidene)tetrahydro-*4H*-thiopyran (4). A suspension of β-hydroxy acid **17** (0.280 g, 0.63 mmol) and *N*,*N*-dimethylformamide dineopentyl acetal (0.58 g, 2.5 mmol, 0.7 mL) in dry CH_3CN (10 mL) was heated at reflux temperature under an inert N_2 atmosphere overnight. The resulting white precipitate was filtered off and recrystallized form hot $CHCl_3$ (40 mL) to afford pure **4** (0.150 g, 0.54 mmol, 62%): mp 213.9 °C; ^{1}H NMR δ 2.25 (s, 8H), 2.53−2.58 (m, 8H), 2.62, 2.67 (m, 8H) ppm; ^{13}C NMR δ 28.9, 30.6, 32.0, 127.7, 130.6 ppm. Anal. Calcd for $C_{16}H_{24}S_2$: C, 68.52; H, 8.62; S, 22.86. Found: C, 68.40; H, 8.70.

Tetrahydro-*4H*-thiopyran-4-on azine (13). To a solution of tetrahydro-*4H*-thiopyran-4-one (**12**, 5.00 g, 43.0 mmol) in CH_3CH_2OH (125 mL) heated at reflux temperature was added dropwise to a solution of $H_2NNH_2\cdot H_2O$ (>99%, 105 mL, 21.6 mmol) in CH_3CH_2OH (50 mL). The reaction mixture was heated at reflux temperature overnight. After cooling to room temperature and removal of solvent in vacuo pure **13** was obtained (4.90 g, 21.5 mmol, 100%): ^{1}H NMR δ 2.66−2.87 (m, 16H) ppm; ^{13}C NMR δ 29.1, 30.2, 30.3, 37.5, 163.5 ppm.

3,7,11-Trithia-14,15-diazadispiro[5.1.5.2]pentadecane (14). A solution of **13** (4.90 g, 21.5 mmol) in CH_3CN (150 mL) was stirred under a H_2S(g) atmosphere (balloon) for 5 days. After evaporation of the solvent in vacuo pure **14** was obtained as a light yellow solid (5.54 g, 21.1 mmol, 98%): ^{1}H NMR δ 2.01−2.13 (m, 8H), 2.65−2.82 (m, 8H), 3.99 (s, 2H) ppm; ^{13}C NMR δ 27.5, 40.5, 85.4 ppm.

3,7,11-Trithia-14,15-diazadispiro[5.1.5.2]pentadec-14-ene (15). Compound **14** (5.54 g, 21.1 mmol) was oxidized with a mixture of $Pb(OAc)_4$ (13.0 g, 29.3 mmol) and $CaCO_3$, (13.0 g, 0.13 mol) in dry CH_2Cl_2 (160 mL).[4a] After work up a brown solid (5.87 g) was obtained, which was recrystallized from hot ethyl acetate to yield pure **15** (3.39 g, 13.0 mmol, 62%):. ^{1}H NMR δ 1.88−1.95 (m, 4H), 2.64−2.93 (m, 12H) ppm; ^{13}C NMR δ 26.4, 40.3, 110.9 ppm.

4-(4-(Tetrahydro-*4H*-thiopyran-4-ylidene)-1-hydroxycyclohexyl)tetrahydro-*4H*-thiopyran-4-carboxylic Acid (17). Tetrahydro-*4H*-thiopyran-4-carboxylic acid (**16**,[12] 0.26 g, 1.80 mmol) and 4-(tetrahydro-*4H*-thiopyran-4-ylidene)cyclohexanone[4a] (0.35 g, 1.80 mmol) were coupled to give the β-hydroxy acid **17** employing a literature procedure.[4a] However, the workup procedure was slightly modified. After the water layer was acidified to ca. pH 1 with concentrated HCl

(37%), it was extracted with $CHCl_3$ (3 × 50 mL). The combined $CHCl_3$ layers were dried ($MgSO_4$), filtered, and concentrated in vacuo. The residue was dried in a vacuum desiccator (P_2O_5) overnight yielding **17** as an off-white solid (0.4 g, 0.87 mmol, 48%): ^{1}H NMR ($CDCl_3$/DMSO-d_6, 1:1) δ 1.44 (m, 2H), 1.72 (m, 4H), 2.11 (m, 2H), 2.4−2.6 (m, 14H), 2.79 (m, 2H) ppm; the COOH and OH protons were not observed; ^{13}C NMR ($CDCl_3$/DMSO-d_6, 1:1) δ 23.9, 25.2, 29.0, 31.1, 32.8, 53.9, 73.1, 125.7, 130.6, 175.9 ppm.

Single-Crystal X-ray Structure Determination of 2. $C_{10}H_{16}S_2$, M = 200.35, colorless needle, 0.50 × 0.08 × 0.08 mm^3, triclinic, $P\bar{1}$ (no 2), a = 5.1689(10) Å, b = 6.2329(12) Å, c = 8.3528(7) Å, α = 72.321(11)°, β = 78.442(11)°, γ = 76.591(15)°, V = 246.94(7) Å^3, Z = 1, d_x = 1.347 g/cm^3, 3682 measured reflections, 1715 unique reflections (R_{int} = 0.0574). μ = 0.48 mm^{-1}. 87 refined parameters, no restraints. $R(I > 2\sigma(I))$: R1 = 0.0387, wR2 = 0.0858. R (all data): R1 = 0.0509, wR2 = 0.0906, S = 1.057. Intensities were measured on a Enraf-Nonius CAD4T diffractometer with rotating anode (Mo Kα, λ = 0.71073 Å) at 150 K up to a resolution of $(\sin\theta\,\lambda^{-1})_{max}$ = 0.74 Å^{-1}. An absorption correction was not considered necessary. The structure was solved with DIRDIF97[33] and refined with SHELXL97[34] against all F^2 of all reflections. Non hydrogen atoms were refined freely with anisotropic displacement parameters. Hydrogen atoms were located in the difference Fourier map and refined freely with isotropic displacement parameters. The drawing, structure calculations and checking for higher symmetry was performed with PLATON.[35]

He(I) Photoelectron Spectroscopy. The He(I) photoelectron (PE) spectra were recorded on a Perkin-Elmer PS 18 spectrometer at the following temperatures: **1**, 60 °C; **2**, 70 °C; **3**, 125 °C; **4**, 60 °C; **5**, 25 °C; **6**, 115 °C; *anti*- and *syn*-**7** 145 °C. The calibration was performed with Ar (15.76 and 15.94 eV) and Xe (12.13 and 13.44 eV). Resolution of 20 meV on the $^2P_{3/2}$ Ar line was obtained.

Calculations

The different conformers of **1**−**6** (C_s: *anti*- and *syn*-**1**, *anti*/*anti*-, *syn*/*anti*- and *anti*/*syn*-**3** and *syn*/*syn*-**3**, *anti*/*syn*-**4** and *anti*/*syn*-**6**, C_{2h}: *anti*-**2**, *anti*-**5**, *anti*/*anti*-**4**, *anti*/*anti*-**6**, *syn*/*syn*-**6** and *anti*-**7** and C_{2v}: *syn*-**2**, *syn*/*syn*-**4**, *syn*-**5** and *syn*-**7**) were optimized at the RHF/6-31G* level of theory using GAMESS-UK.[36] In addition, *anti*-**1** (C_s), *anti*-**2** (C_{2h}), and *syn*-**2** (C_{2v}) were also optimized at the RHF/6-311G** level of theory. Hessian calculations revealed that all conformers represent genuine minima (see Supporting Information).

The NBO analyses were performed using the NBO 3.0 program.[37]

Acknowledgment. We thank A. Flatow for recording the PE spectra. R.G. is grateful to the Deutsche Forschungsgemeinschaft, the Volkswagenstiftung, the Fonds der Chemischen Industrie, and the BASF Aktiengesellschaft for financial support. Partial financial support (M.L., A.L.S.) by the Council for Chemical Sciences of The Netherlands Organization for Scientific Research (NWO-CW) is also gratefully acknowledged.

Supporting Information Available: Cartesian coordinates of the RHF/6-31G*-optimized geometries of all conformers of **1**−**7** as well as Cartesian coordinates of the RHF/6-311G**-optimized geometries of *anti*-**1**, *anti*-**2**, and *syn*-**2**. Calculated RHF/6-31G* molecular orbital (MO) energies and MO assignments of *anti*/*syn*-**3**, *syn*/*anti*-**3**, *syn*/*syn*-**3**, *anti*/*syn*-**4**, and *syn*/*syn*-**4** (Table 1). Single-crystal X-ray structural data of **2**. This material is available free of charge via the Internet at http://pubs.acs.org.

JO000199Y

(33) Beurskens, P. T.; Admiraal, G.; Beurskens, G.; Bosman, W. P.; Garcia-Granda, S.; Gould, R. O.; Smits, J. M. M.; Smykalla, C. *The DIRDIF97 Program System, Technical Report of the Crystallographic Laboratory*; University of Nijmegen: The Netherlands, 1997.

(34) Sheldrick, G. M. SHELXL97, *Program for Crystal Structure Refinement*; University of Göttingen: Germany, 1997.

(35) Spek, A. L. *PLATON, A Multipurpose Crystallographic Tool*; Utrecht University: The Netherlands, 1999.

(36) GAMESS-UK is a package of ab initio programs written by: Guest, F.; van Lenthe, J. H.; Kendrick, J.; Schoffel, K.; Sherwood, P.; Harrison, R. J. 1998 with contributions from: Amos, R. D.; Buenker, R. J.; Dupuis, M.; Handy, N. C.; Hiller, I. H.; Knowles, P. J.; Bonacic-Koutecky, V.; Niessen, W.; Saunders: V. R.; Stone, A. J. The package is derived from the original GAMESS code due to: Dupuis, M.; Spangler, D.; Wendolowski, J., *NRCC Software Catalog*, Vol 1, Program No. QG01 (GAMESS) **1980**.

(37) NBO 3.0 program: *Natural Bond Orbital*/*Natural Population Analysis*/*Natural Localized Molecular Orbitals Program*, Glendering, E. D.; Reed, A. E.; Carpenter, J. E.; Weinhold, F. as implemented in GAMESS-UK (see also ref 27).[36]